Enumeration of Optimal Pin-Jointed Bistable Compliant Mechanisms with Non-Crossing Members

M. Ohsaki, N. Katoh, T. Kinoshita, S. Tanigawa, D. Avis and I. Streinu

Abstract An optimization approach is presented for enumerating pin-jointed bistable compliant mechanisms. In the first stage, the statically determinate trusses with non-crossing members containing a given set of nodes and some pre-defined members are regarded as minimally rigid framework or a Laman framework, and are enumerated without repetitions by the graph enumeration algorithm. In the second stage, the nodal locations and the cross-sectional areas are optimized under mechanical constraints, where the snapthrough behavior is extensively utilized to produce a pin-jointed bistable compliant mechanism. In the numerical examples, many bistable compliant mechanisms are generated to show the effectiveness of the proposed method.

Key words Bistable structure, Compliant mechanism, Minimally rigid framework, Snapthrough

1
Introduction

Contrary to unstable conventional bar–joint mechanisms, a *compliant mechanism* utilizes elastic deformation of structural parts to realize a mechanism for producing a large output displacement in the different direction from the input displacement (Larsen *et al.* 1996). Pedersen *et al.* (2002) incorporated the effect of large deformation in the optimization process.

Recently, optimization considering geometrically nonlinear buckling has been extensively studied (Ohsaki 2005;

M. Ohsaki[1], N. Katoh[1], T. Kinoshita[1], S. Tanigawa[1], D. Avis[2] and I. Streinu[3]

[1] Department of Architecture and Architectural Engineering, Kyoto University, Kyotodaigaku-Katsura, Nishikyo, Kyoto 615-8540, Japan
e-mail: ohsaki@archi.kyoto-u.ac.jp   [2] School of Computer Science, McGill University, Canada
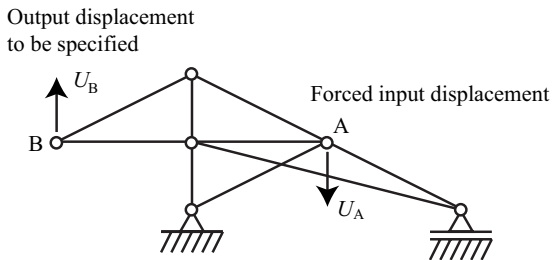[3] Dept. of Computer Science, Smith College, Northampton, MA 01063, USA

Ohsaki and Ikeda 2007). Bruns and Sigmund (2004) utilized snapthrough behavior to generate a large deformation that can lead to a bistable structure with two stable self-equilibrium states (Masters and Howell 2003).

Although a compliant mechanism is usually designed as continuum (Nishiwaki *et al.* 2001), it is also possible to use flexibility of members of a bar–joint mechanism. Ohsaki and Nishiwaki (2005) presented an optimization algorithm for generating multistable compliant bar–joint mechanisms, where a ground structure approach is used and the design variables of the optimization problem are the cross-sectional areas of members and the nodal coordinates of a truss. In their method, bistability is achieved using the snapthrough behavior and an obstacle to terminate the displacement of input node. Mankame and Ananthasuresh (2004a) also presented a contact-aided compliant mechanism. However, in their method, the contact is used for changing the mode of deformation, and geometrical nonlinearity or bistability is not considered. Prasad and Diaz (2006) developed a ground structure approach using nonlinear beam elements to generate bistable periodic frame structures. Optimization is carried out by genetic algorithms. A frame model is also used by Mankame and Ananthasuresh (2004b).

Since a pin-jointed compliant mechanism is usually statically determinate, a variety of mechanisms of different types for specified input-output relation can be generated by enumerating the initial statically determinate structures for the optimization problem. Enumeration is not a new idea in the field of the design of mechanisms. The process of designing mechanisms is usually divided to 'type synthesis,' 'number synthesis' and 'dimensional synthesis.' For number synthesis, many methods have been developed for enumerating the basic kinematic chains with specified numbers of links and degrees of freedom; e.g., Tuttle *et al.* (1989). However, more straightforward approach is desired to avoid the complicated three-step approach.

Kawamoto *et al.* (2004) developed a design method for link mechanisms based on graph theoretical enumeration. In their method, a subset of nodes is first defined from the candidate nodes, and the set of members with specified number is enumerated based on the bipartite matching problem between vertices and edges in graph

Fig. 1 Input and output displacements of a pin-jointed compliant mechanism.

Fig. 2 A two-bar truss.

Fig. 3 Input force-displacement relation of the two-bar truss.

theory. However, the computational cost for the enumeration increases as an exponential function of the number of nodes.

Saxena and Ananthasuresh (2003) developed a design method of compliant mechanism using a ground structure approach with beam elements. The compliant frame mechanism is transformed to an equivalent kinematic chain. This way, number synthesis and dimensional synthesis are simultaneously carried out by optimization, and different kinematic chains can be generated from different compliant mechanisms. However, they did not present a systematic approach to enumeration of mechanisms. Furthermore, geometrical nonlinearity or bistability has not been considered.

In this paper, we propose a computationally efficient approach based on new enumeration method of statically determinate trusses without crossing members to find many types of compliant mechanisms.

2
Pin-jointed bistable compliant mechanism

Consider a structure as shown in Fig. 1. A pin-jointed bistable compliant mechanism is defined as follows:

1. A large displacement U_B is generated at output node 'B' in the specified direction as a result of forced displacement U_A at input node 'A'.
2. The deformed states can be retained without external loads; i.e., the structure has two self-equilibrium states including the undeformed initial state.
3. The structure has moderately large stiffness at the initial state, and at the final state after constraining the input degree-of-freedom.
4. The undeformed initial state can be recovered by reversely applying a small force as a disturbance at the deformed final state.

For a two-bar truss as shown in Fig. 2, the bistable structure can be realized by utilizing the snapthrough behavior, where the dotted and solid lines in Fig. 2 are the shapes before and after deformation, respectively. Fig. 3 illu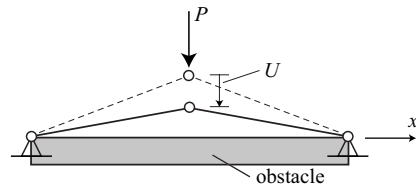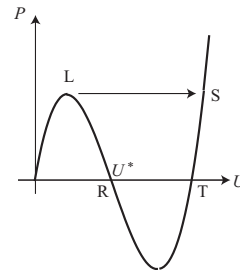strates the relation between the forced input displacement U and the input force (reaction) P. The input force P increases until reaching the limit point 'L', and decreases if U is further increased beyond the limit point. If the deformation is controlled by P, the equilibrium state jumps from 'L' to 'S' by a dynamic behavior called snapthrough. Let U^* denote the value of U at 'R' in Fig. 3 satisfying $P = 0$ beyond the limit point, when the two bars are colinear in the horizontal position. Suppose an obstacle is placed at 'R' as shown in Fig. 2. Note that this equilibrium state can be stabilized by a small additional force against the obstacle, or by placing the obstacle slightly below the horizontal line between the two supports. This way, a bistable mechanism that has self-equilibrium states $U = 0$ and $U \simeq U^*$ can be generated.

Ohsaki and Nishiwaki (2005) presented a ground structure approach to generate a pin-jointed compliant mechanisms. However their method is not practically acceptable because,

1. Nonlinear programming from randomly selected initial solutions should be carried out many times to reach a few candidates for the mechanisms, because the analysis and optimization problems are highly nonlinear and many members should be removed from the highly connected ground structure.
2. There exist crossing members that are difficult to manufacture.

Since a pin-jointed compliant mechanism is stable, a statically determinate truss can realize a compliant mechanism with the minimum number of members for a given set of supports and input- output-nodes. Therefore, we first enumerate the statically determinate trusses
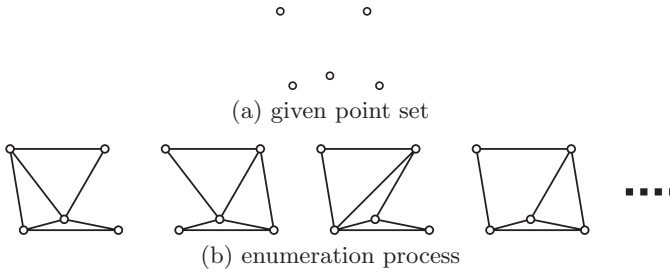
(a) given point set

(b) enumeration process

Fig. 4 Illustration of enumerating process.

without crossing members, and solve an optimization problem for each topology.

3
Graph enumeration

In graph theory, a statically determinate truss having no intersecting members is regarded as a *planar embedded minimally rigid graph* or *non-crossing Laman framework* (Graver *et al.* 1993). Let $G = (V, E)$ be a graph with $n = |V|$ vertices and $m = |E|$ edges. G is a *minimally rigid graph* (also called *Laman graph*) if $m = 2n - 3$ and every subset of $n' \leq n$ vertices spans at most $2n' - 3$ edges. An embedding $G(\boldsymbol{p})$ of the graph G on a set of points $\boldsymbol{p} = \{p_1, \cdots, p_n\} \subset R^2$ is a mapping of the vertices V to points in the Euclidean plane $i \mapsto p_i \in \boldsymbol{p}$. The edges $ij \in E$ are mapped to straight line segments $p_i p_j$. An embedding $G(\boldsymbol{p})$ is *non-crossing* if no pair of segments $p_i p_j$ and $p_k p_l$ corresponding to non-adjacent edges $ij, kl \in E, i, j \notin \{k, l\}$ have a point in common. Laman graphs embedded on *generic* point sets are called *Laman frameworks* or *minimally rigid frameworks*.

In our recent paper (Avis *et al.* 2007), an efficient algorithm was developed for enumerating without repetitions all the non-crossing Laman frameworks on a given point set in the plane using little memory based on the reverse search technique developed by Avis and Fukuda (1996). The reverse search is well known technique to generate all the elements of the combinatorial objects without memorizing objects that are already enumerated by tracing the nodes in the search graph, where search graph is the graph each of whose node corresponds to each object to be enumerated and edge corresponds to a transformation between two connected elements. By appropriately defining the root which is a special object and the parent for each object except the root, the algorithm traces the search tree in a depth-first manner induced by the parent-child relation to enumerate all objects without repetitions. For example, given a point set in the plane, see Fig. 4(a), our enumeration algorithm finds all the non-crossing minimally rigid frameworks without repetitions, see Fig. 4(b).

However, it is known that the number of non-crossing Laman frameworks grows too rapidly to allow a complete enumeration for significantly larger examples. Consid-

ering that the optimal structure should always contain some *pre-defined members*, the computational cost could be much reduced if the candidate set of non-crossing Laman frameworks is restricted to the one containing pre-defined edge set. In Avis *et al.* (2006a), we have developed an algorithm for enumerating without repetitions all the non-crossing Laman frameworks containing a specified edge set in the plane. Our algorithm generates each output graph in $O(n^3)$ time and $O(n^2)$ space also based on the reverse search technique, where n is the number of points.

4
Problem Formulation

We solve a nonlinear programming problem for each topology generated by the enumeration.

Let a superscript $(\cdot)^{\mathrm{f}}$ denote the value at the final state, which is defined so that the displacement $U_{\mathrm{B}}^{\mathrm{f}}$ of the output node 'B' reaches the specified value $\bar{U}_{\mathrm{B}}$ as $U_{\mathrm{B}}^{\mathrm{f}} = \bar{U}_{\mathrm{B}}$. The final state can also be defined by the distance of the two output nodes as described in the examples. Let a superscript $(\cdot)^0$ denote the response against a unit load. The displacement U_{A}^0 computed using the linear stiffness matrix against the unit input load at the initial state should be less than the upper bound $\bar{U}_{\mathrm{A}}^0$. The displacements $U_{\mathrm{B}x}^{\mathrm{f}0}$ and $U_{\mathrm{B}y}^{\mathrm{f}0}$ computed by the linear stiffness matrix against the unit loads in x- and y-directions at the output node after constraining the input degree-of-freedom at the final state should be less than the upper bounds $\bar{U}_{\mathrm{B}x}^{\mathrm{f}0}$ and $\bar{U}_{\mathrm{B}y}^{\mathrm{f}0}$, respectively. This way, the stiffness of the mechanism is ensured.

The variables are the vectors of cross-sectional areas $\boldsymbol{A}$ and the nodal coordinates $\boldsymbol{X}$. A bistable mechanism is generated by minimizing the absolute value $|P_{\mathrm{A}}^{\mathrm{f}}|$ of the input load at the final state. Hence, the optimization problem is formulated as

minimize $\quad |P_{\mathrm{A}}^{\mathrm{f}}(\boldsymbol{A}, \boldsymbol{X})| \quad$ (1a)

subject to $\quad U_{\mathrm{A}}^0 \leq \bar{U}_{\mathrm{A}}^0 \quad$ (1b)

$\quad U_{\mathrm{B}x}^{\mathrm{f}0}(\boldsymbol{A}, \boldsymbol{X}) \leq \bar{U}_{\mathrm{B}x}^{\mathrm{f}0} \quad$ (1c)

$\quad U_{\mathrm{B}y}^{\mathrm{f}0}(\boldsymbol{A}, \boldsymbol{X}) \leq \bar{U}_{\mathrm{B}y}^{\mathrm{f}0} \quad$ (1d)

$\quad \boldsymbol{A}^{\mathrm{L}} \leq \boldsymbol{A}, \quad \boldsymbol{X}^{\mathrm{L}} \leq \boldsymbol{X} \leq \boldsymbol{X}^{\mathrm{U}} \quad$ (1e)

where $\boldsymbol{A}^{\mathrm{L}}$ is the lower bound for $\boldsymbol{A}$, and $\boldsymbol{X}^{\mathrm{L}}$ and $\boldsymbol{X}^{\mathrm{U}}$ are the lower and upper bounds for $\boldsymbol{X}$, respectively.

Note that the lower bound $\boldsymbol{A}^{\mathrm{L}}$ may be moderately large, because topology is fixed and no removal of members should be considered. This way, convergence property of optimization is significantly improved from the previous method in Ohsaki and Nishiwaki (2005) that allows removal of members. The bounds for the displacements can also be easily assigned. $\bar{U}_{\mathrm{A}}^0$ is given according to the geometry of the truss and the design requirement. Arbitrary positive same value can be assigned for $\bar{U}_{\mathrm{B}x}^{\mathrm{f}0}$
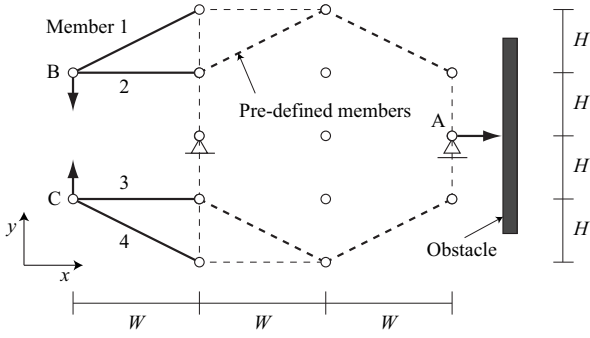
4

Fig. 5 Initial set of nodes and supports for generating mechanisms.

(a) Set of nodes with no member specified.   (b) Set of nodes with Pre-selected members.
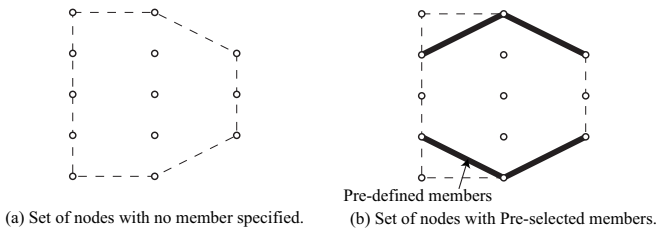
Fig. 6 Sets of nodes for enumeration of non-crossing Laman frameworks.

and $\bar{U}_{\mathrm{B}y}^{\mathrm{f}0}$, because they only affect the scale of the cross-sectional areas; i.e., the cross-sectional areas are inversely proportional to the value of $\bar{U}_{\mathrm{B}x}^{\mathrm{f}0}$ and $\bar{U}_{\mathrm{B}y}^{\mathrm{f}0}$.

The optimization algorithm is summarized as

Step 1: Select a topology from the list obtained by graph enumeration. Assign random initial values to $\boldsymbol{A}$ and $\boldsymbol{X}$.
Step 2: Trace the equilibrium path by adopting the input displacement U_{A} as the path parameter.
Step 3: Go to Step 1 if U_{B} at the first incremental step is opposite to $U_{\mathrm{B}}^{\mathrm{f}}$. Otherwise, trace the path until reaching the final state.
Step 4: Compute sensitivity coefficients of the objective and constraint functions with respect to $\boldsymbol{A}$ and $\boldsymbol{X}$.
Step 5: Update $\boldsymbol{A}$ and $\boldsymbol{X}$ in accordance with an optimization algorithm.
Step 6: Go to Step 2 if the iteration does not converge.
Step 7: Go to Step 1 to find another mechanism.

5
Examples of bistable compliant mechanisms

Numerical examples are presented to confirm the effectiveness of the proposed method. A PC with Intel Xeon 3.4 GHz CPU and 2GB RAM is used for computation.

Various types of bistable grippers that can achieve self-equilibrium states at both deformed and undeformed states are generated from the set of nodes and supports as shown in Fig. 5, where $W = 0.2$ m and $H = 0.1$ m. The equipment can control the gap between the output nodes 'B' and 'C' to grip a workpiece without external loads by the forced displacement in x-direction at the input node 'A'.

Members 1–4 are considered as gripping arms and excluded from design region. Therefore, the mechanisms are generated with the 13 nodes connected by members located inside or along the boundary of the convex design region defined by the dotted lines in Fig. 6(a). The four thick dotted lines in Fig. 5 are the pre-defined necessary members. If we do not specify the four necessary members, the number of frameworks enumerated by our previous method in Avis et al. (2007) is 1027992, and the CPU time for enumeration is 34667 sec. If we specify the necessary members in view of practical requirement as shown in Fig. 6(b), the number of frameworks and CPU time are drastically reduced to 68072 and 2138 sec., respectively, by using the algorithm in Avis et al. (2006a).

In the second stage, the bars are modeled as pin-jointed truss members. The final state is defined such that the distance between nodes 'B' and 'C' decreases from $2H$ to H. Other parameters are $\bar{U}_{\mathrm{A}}^{0} = \bar{U}_{\mathrm{B}x}^{\mathrm{f}0} = \bar{U}_{\mathrm{B}y}^{\mathrm{f}0} = 0.05$ m, where the unit of force is kN. Elastic modulus is 200.0 N/mm^2 and the rotated engineering strain is used for the definition of strain-displacement relation. The equilibrium path is traced by the displacement increment method, where the input displacement is used as the path-parameter with the increment 0.0002 m. This way, the equilibrium path is traced without any trouble through the limit point. No Newton-Raphson iteration is carried out, and the unbalanced loads are canceled at the following step. Only the linear stiffness matrix at the current deformed configuration is used for the linear estimate of the incremental displacements; otherwise it is very difficult to prevent divergence of the incremental solution due to existence of thin members. The accuracy of the analysis program has been verified in Ohsaki and Nishiwaki (2005) by comparing the results with ANSYS Ver. 7.0. It is also verified in the following examples that the norm of the unbalanced loads is very small compared with that of the applied load.

Optimization is carried out by IDESIGN Ver. 3.5 (Arora and Tseng 1987), where the sequential quadratic programming is used. The cross-sectional areas of all members are independent variables with lower bound 1.0×10^{-6} m^2. The coordinates of nodes 'B', 'C' and the supports are fixed during optimization. Let x_i^0 denote the x-coordinate of an unconstrained node in the original geometry in Fig. 5. The upper and lower bounds of x_i are given by $x_i^0 \pm 0.02$ m. The feasible regions of the y-coordinates y_i with original location y_i^0 are defined similarly. The same initial values are given for optimization of each topology, i.e., $A_i = 1.0 \times 10^{-4}$, $x_i = x_i^0$, $y_i = y_i^0$.

By carrying out optimization from 68072 initial solutions, we found 156 different types of mechanisms. Note that 51336 solutions are rejected before carrying out optimization, because the distance between the two out-
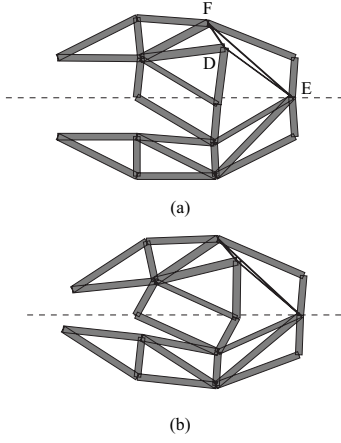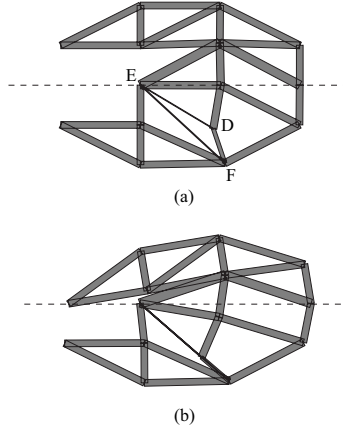
Fig. 7 Optimal topology (Type-1).

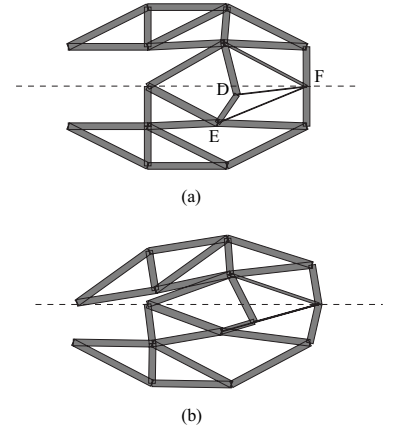Fig. 8 Optimal topology (Type-2).

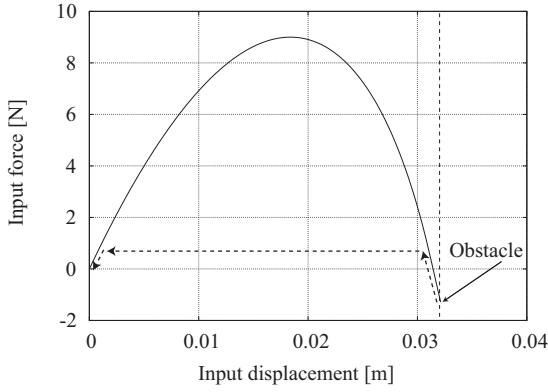Fig. 9 Optimal topology (Type-3).

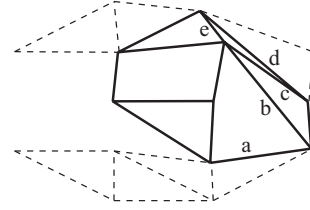Fig. 10 Relation between the input displacement and load of Type-1.

Fig. 12 Deformed part of Type-1.

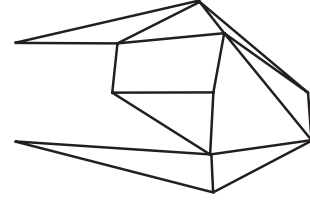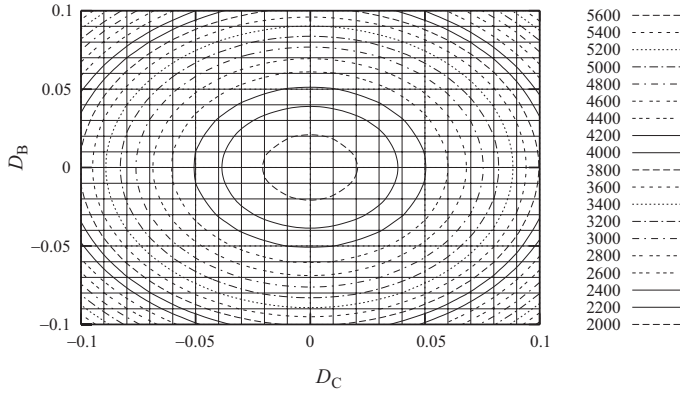Fig. 13 Simplified shape of of Type-1.

Fig. 11 Contour map of the total potential energy with respect to D_B and D_C at the final state.

found from randomly generated 100 initial solutions in Ohsaki and Nishiwaki (2005). Therefore, computational cost has been significantly reduced by the proposed method. Figs. 7–9 show three typical solutions, where (a) is the optimal topology, and (b) is the deformed final shape. It is seen that the triangle formed by the three nodes 'D', 'E' and 'F' buckles to form three colinear members for each topology in Figs. 7–9 to realize the snapthrough behavior. These triangles are located in different places, and it would be very difficult to find these mechanisms by intuition; i.e., the effectiveness of the proposed method has been successfully demonstrated. Fig. 10 shows the the relation between the force P_A and the displacement U_A at the input node. Note that the input force decreases to a slightly negative value and deformation terminates with the contact of the input node to the obstacle plated at $U_A = 0.032$.

Let D_B and D_C denote the incremental displacements in the y-direction at the output nodes B and C, respectively. To verify the stability of the final state, the contour map of the total potential energy Π is plotted in

put nodes 'B' and 'C' increases as the input displacement is increased; i.e., there is little possibility of finding the desired mechanisms from such initial solutions. The number of iterations in optimization for the converged solution is about 20, whereas it is more than 50 in the topology optimization approach in Ohsaki and Nishiwaki (2005). Furthermore, only three solutions were

Fig. 11. If Π increases for any admissible increment of displacements, then the equilibrium state is stable. At the final state, where the input node contacts with the obstacle with non-zero contact force, the admissible incremental displacements are given such that the input node and the obstacle remain in contact state (Klarbring 1988). As is seen in Fig. 11, Π takes the minimum value at the final equilibrium state with $D_B = D_C = 0$. It has been confirmed that the tangent stiffness after constraining the input degree-of-freedom at the final state is positive definite. Since similar plots are obtained for any admissible incremental displacements, the final state is stable, and the initial state is easily recovered by applying small reverse load to the input node as illustrated in the dotted arrows in Fig. 10, because the contact force at the final state is sufficiently small.

The solid lines in Fig. 12 are the members that have moderately large strains in Type-1 solution. The maximum absolute values of the strains in members 'a'–'e' are 2.4252×10^{-4}, 7.9532×10^{-4}, 4.0123×10^{-4}, 6.4626×10^{-3} and 1.7835×10^{-3}, respectively. The remaining parts with dotted lines can be replaced with arbitrary rigid framework as shown in Fig. 13.

6
Conclusions

An optimization approach has been presented for the design of pin-jointed compliant mechanisms. In the first stage, non-crossing Laman frameworks, which are equivalent to statically determinate bar–joint structures, are enumerated by using the algorithm developed by the authors, where the necessary edges (members) are explicitly specified. This way, the total number of enumerated frameworks and the computational time for enumeration can be drastically reduced.

In the second stage, many bistable compliant mechanisms are generated from the initial solutions obtained in the first stage. It has been shown in the numerical examples that many practically acceptable mechanical grippers undergoing large deformation and bistability can be found by the proposed method. The snapthrough behavior has been confirmed to be realized by the local buckling of the triangular elements.

References

Arora, J. S. and Tseng, C. H. (1987). Idesign user's manual, ver. 3.5. Technical report, Optimal Design Laboratory, The University of Iowa.

Avis, D. and Fukuda, K. (1996). Reverse search for enumeration. *Discrete Applied Math.*, **65**(1–3), 21–46.

Avis, D., Katoh, N., Ohsaki, M., Streinu, I., and Tanigawa, S. (2006a). Enumerating constrained non-crossing minimally rigid frameworks. *Discrete and Computational Geometry*. to appear; also available at: http://arxiv.org/abs/math/0608102v2.

Avis, D., Katoh, N., Ohsaki, M., Streinu, I., and Tanigawa, S. (2007). Enumerating non-crossing minimally rigid frameworks. *Graphs and Combinatorics*, **23(Suppl)**, 117–134.

Bruns, T. E. and Sigmund, O. (2004). Toward the topology design of mechanisms that exhibit snap-through behavior. *Comp. Meth. Appl. Mech. Engng.*, **193**, 3973–4000.

Graver, J., Servatius, B., and Servatius, H. (1993). *Combinatorial Rigidity*. Graduate Studies in Mathematics Vol. 2.

Kawamoto, A., Bendsøe, M. P., and Sigmund, O. (2004). Planar articulated mechanism design by graph theoretical enumeration. *Structural Optimization*, **27**, 295–299.

Klarbring, A. (1988). On discrete and discretized non-linear elastic structures in unilateral contact (stability, uniqueness and variational principles). *Int. J. Solids Struct.*, **24**(5), 459–479.

Larsen, U. D., Sigmund, O., and Bouwstra, S. (1996). Design and fabrication of compliant micromechanisms and structures with negative poisson's ratio. In *Proc. IEEE 9th Annual Int. Workshop on Micro Electro Mech. Sys., An Investigation of Micro Structures, Sensors, Actuators, Machines and Systems*, pages 365–371, San Diego, California.

Mankame, N. D. and Ananthasuresh, G. K. (2004a). Topology optimization for synthesis of contact-aided compliant mechanisms using regularized contact modeling. *Comp. & Struct.*, **82**, 1267–1290.

Mankame, N. D. and Ananthasuresh, G. K. (2004b). Topology synthesis of electrothermal compliant mechanisms using line elements. *Struct. Multidisc. Optim.*, **26**, 209–218.

Masters, N. D. and Howell, L. L. (2003). A self-retracting fully compliant bistable micromechanism. *J. MEMS*, **12**, 273–280.

Nishiwaki, S., Min, S., Yoo, J., and Kikuchi, N. (2001). Optimal structural design considering flexibility. *Comp. Meth. Appl. Mech. Engng.*, **190**, 4457–4504.

Ohsaki, M. (2005). Design sensitivity analysis and optimization for nonlinear buckling of finite-dimensional elastic conservative structures. *Comp. Meth. Appl. Mech. Engng.*, **194**, 3331–3358.

Ohsaki, M. and Ikeda, K. (2007). *Stability and Optimization of Structures – Generalized Sensitivity Analysis*. Mechanical Engineering Series. Springer, New York.

Ohsaki, M. and Nishiwaki, S. (2005). Shape design of pin-jointed multistable compliant mechanism using snapthrough behavior. *Structural Optimization*, **30**, 327–334.

Pedersen, C. B. W., Buhl, T., and Sigmund, O. (2002). Topology optimization of large-displacement compliant mechanisms. *Int. J. Num. Meth. Engng.*, **44**, 1215–1237.

Prasad, J. and Diaz, A. R. (2006). Synthesis of bistable periodic structures using topology optimization and a genetic algorithm. *J. of Mechanical Design, ASME*, **128**, 1298–1306.

Saxena, A. and Ananthasuresh, G. K. (2003). A computational approach to the number synthesis of linkages. *J. of Mechanical Design, ASME*, **125**, 110–118.

Tuttle, E. R., Peterson, S. W., and Titus, J. E. (1989). Enumeration of basic kinematic chains using the theory of finite groups. *J. of Mechanisms, Transmissions, and Automation in Design, ASME*, **111**, 498–503.